AD-A087 733 MARYLAND UNIV COLLEGE PARK DEPT OF PHYSICS AND ASTRONOMY F/G 20/7
PLASMA INSTABILITY IN ELECTRON AND POSITRON COLLIDING BEAMS IN --ETC(U)
APR 80 H S UHM, C S LIU N00014-77-C-0590
UNCLASSIFIED PUB-80-180 NL

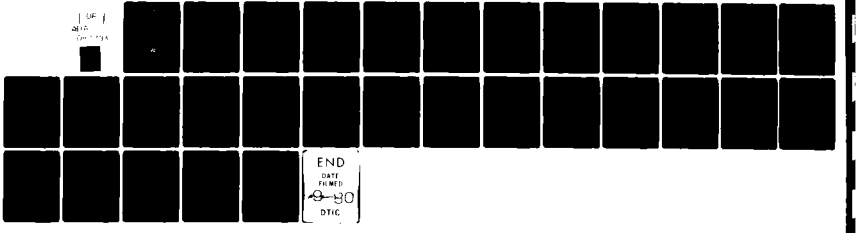

END
DATE FILMED
9-80
DTIC

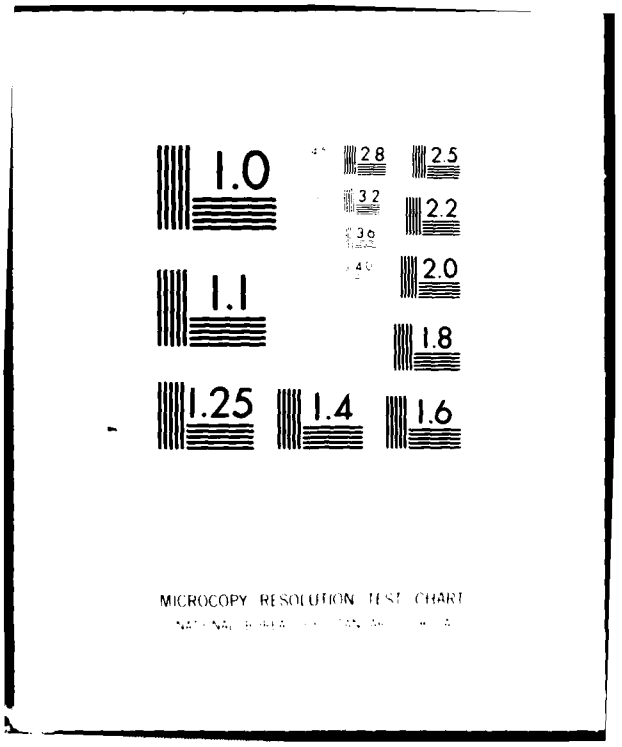
1.0
2.8
2.5
3.2
2.2
3.6
4.0
2.0
1.1
1.8
1.25
1.4
1.6
MICROCOPY RESOLUTION TEST CHART

LEVEL II

Plasma Preprint PL #80-040

PLASMA INSTABILITY IN ELECTRON AND POSITRON COLLIDING BEAMS IN STORAGE RING

Han S. Uhm
Naval Surface Weapons Center
White Oak, Silver Spring, Maryland 20910

and

Chuan S. Liu
Department of Physics and Astronomy
University of Maryland
College Park, Maryland 20742

Physics Publication Number 80-180
Technical Report Number 80-103

April 1980

UNIVERSITY OF MARYLAND
DEPARTMENT OF PHYSICS AND ASTRONOMY
COLLEGE PARK, MARYLAND

Plasma Preprint PL #80-040

PLASMA INSTABILITY IN ELECTRON AND POSITRON COLLIDING BEAMS IN STORAGE RING

Han S. Uhm
Naval ~~Surface Weapons~~ Center
White Oak, Silver Spring, Maryland 20910

and

Chuan S. Liu
Department of Physics and Astronomy
University of Maryland
College Park, Maryland 20742

N00014-77-C-0590

Physics Publication Number 80-180
Technical Report Number 80-103

April 1980

PLASMA INSTABILITY IN ELECTRON AND POSITRON COLLIDING BEAMS IN STORAGE RING

Han S. Uhm
Naval Surface Weapons Center
White Oak, Silver Spring, Maryland 20910

and

Chuan S. Liu
Department of Physics and Astronomy
University of Maryland
College Park, Maryland 20742

ABSTRACT

The filamentation instability of the electron and positron colliding beams in a storage ring are investigated within the framework of the rigid beam model and the Vlasov-Maxwell equations, and closed algebraic dispersion relations for the complex eigenfrequency ω are obtained. It is shown that the typical growth rate of instability is a substantial fraction of the electron plasma frequency ω_{pe}, thereby severely limiting the electron density in a storage ring. Moreover, the influence of collective self-field effects on the electron and positron colliding beams in the storage ring is investigated. The analysis is carried out, distinguishing the cases, where (a) the particle motions are in a very coherent orbit, and (b) the randomness dominates the operational condition of a storage ring (e.g., the incoherent collision location by small fluctuation, etc.) In

either case, it is shown that the self-fields effects play a dominant role in the stability behavior of transverse orbit or the expansion of the beam cross section.

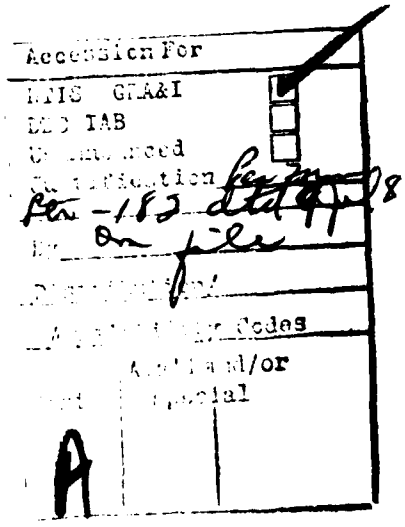

INTRODUCTION

There is a growing interest in the equilibrium and stability properties of the electron-positron colliding beams in a storage-ring facility.[1-3] A recent experiment[4] with colliding electron-positron beams at DESY has shown the broadening of the beam cross section, thereby leading to reduction of luminosity. To address this serious problem, we examine the filamentation instability[3] of electron-positron beams and the influence of the collective self-field[5] on the electron-positron colliding beams in the storage ring. For the analytic simplicity, we assume that beams have cylindrical shape and are azimuthally symmetric in the equilibrium state. Equilibrium and stability properties of planar geometric beams are to be presentd in a subsequent publication.

In Sec. II, we treat the filamentation instability[3] of colliding electron-positron beams with finite-geometry effects included. Stability analysis of dipole oscillation is carried out in Sec. II.A, within the framework of a rigid beam model, which provides a simple instructive description. In Sec. II.B, the analysis for the high harmonic perturbations with $\ell \geq 2$ (where ℓ is azimuthal harmonic number) is carried out within the framework of the Vlasov-Maxwell equations. An important conclusion of the present analysis is that the typical growth rate of the filamentation instability is of the order of the electron plasma frequency ω_{pe}, thereby severely limmiting the electron density in a storage ring. However, the analysis of broadening of beam cross section by repeating interaction between electron and positron beams is not completed yet.

The influence of the collective self-fields[5] on the electron and positron colliding beams in the storage ring is investigated in Sec. III. The

theoretical analysis is carried out, distinguishing the two cases, where (a) the particle motions are in a very coherent orbit and (b) the randomness dominates the operational condition of storage ring (e.g., incoherent collision location by fluctuation, etc.). In either case, it has been found that the self-fields effects play a dominant role in the stability behavior of transverse orbit and the expansion of beam cross section.

II. FILAMENTATION INSTABILITY

Electron and positron colliding beams in storage ring are likely subject to various macro- and micro-instabilities.[3,6] Perhaps one of the most important instabilities of the electron and positron colliding beam in a storage ring is the filamentation instability. The unstable modes propogates nearly perpendicular to the beam with mixed electrostatic and electromagnetic components, the latter destabilizing and the former stabilizing. The perturbed magnetic field is mostly in the plane perpendicular to the beam and the Lorentz force causes the beam to filamentate, similar to the Weibel instability. Unlike the Weibel modes, which are purely electromagnetic for counter-streaming electron beams, the linear perturbations of colliding electron-positron beams cause both charge and current perturbations giving rise to mixed polarizations. Furthermore, for the case of colliding-beams with radial dimension smaller than the collisionless skin depth c/ω_p, the finite geometry becomes important and the usual assumption of infinite, homogeneous medium is no longer valid. In this paper, we treat the filamentation instability of colliding electron-positron beams with finite geometry effects included. For simplicity, we assume in this section that this colliding beam is straight and infinite along the axial direction.

The analysis is carried out within the framework of both the rigid beam model and the Vlasov-Maxwell equations. As illustrated in Fig. 1, the equilibrium configuration consists of intense relativistic electron and positron beams propagating opposite to each other with axial velocity $\beta_p c \hat{e}_z$ for the positron beam and $\beta_e c \hat{e}_z$ for the electron beam, where $\hat{e}_z$ is a unit vector along the z-direction and c is the speed of light in

vacuo and $\beta_p=-\beta_e$. Moreover, both beams have the same radius R_b and the same characteristic energy $\gamma_b mc^2$. It is also assumed that the ratio of the beam radius to the collisionless skin depth c/ω_p is small, i.e.,

$$\frac{\nu_j}{\gamma_b} = N_j \frac{e^2}{mc^2}\frac{1}{\gamma_b} << 1 \quad , \tag{1}$$

where j=e,p denote electrons and positrons, respectively, ν_j is Budker's parameter, $N_j = 2\pi \int_0^\infty dr\, r\, n_j^0(r)$ is the number of particles per unit axial length, $n_j^0(r)$ is the equilibrium particle density of beam component j, -e and m are the charge and rest-mass, respectively, of electron. As shown in Fig. 1, we introduce a cylindrical polar coordinate system (r,θ,z). All equilibrium properties are assumed to be azimuthally symmetric $(\partial/\partial\theta=0)$ and independent of axial coordinate $(\partial/\partial z=0)$.

A. Rigid Beam Model

In order to illustrate the physical mechanism of this filamentation instability, we carry out the stability analysis in this section within the framework of a "rigid beam" model. For the purpose of analytic simplication, we also specialize to the case of sharp-boundary profiles in which the equilibrium density profiles are rectangular, i.e.,

$$n_j^0(r) = \begin{cases} \hat{n}_j = \text{const}, & 0<r<R_b, \\ 0, & \text{otherwise}, \end{cases} \tag{2}$$

where j=e and p. Making use of Eq. (2), it is straightforward to show that the equilibrium radial electron field produced by particles of species j is given by

$$E_{jr}(r) = \begin{cases} 2\pi e_j \hat{n}_j r , & 0<r<R_b , \\ 2\pi e_j \hat{n}_j R_b^2/r , & r>R_b , \end{cases} \tag{3}$$

where e_j is the charge of particles of beam component j (i.e., $e_j=-e$ for j=e and $e_j=e$ for j=p). Similarly, the equilibrium azimuthal magnetic field produced by particles of species j can be expressed as

$$B_{j\theta}(r) = \begin{cases} 2\pi e_j \hat{n}_j \beta_j r , & 0<r<R_b , \\ 2\pi e_j \hat{n}_j \beta_j R_b^2/r , & r>r_b , \end{cases} \tag{4}$$

where $V_j=\beta_j c$ is the axial drift velocity and c is the speed of light in vacuo.

In the subsequent analysis, we introduce the center of mass coordinates (X_j,Y_j) for the beam component of specis j. In the equilibrium state, we assume that

$$(X_j,Y_j) = (0, 0) , \tag{5}$$

for j=e, and p. It is also assumed that

$$X_j^2 + Y_j^2 << R_b^2 . \tag{6}$$

The restriction to small perturbation amplitudes makes the subsequent stability analysis tractable. The transverse motion of a single particle of species j is determined approximately from

$$m_j \frac{d^2}{dt^2} \underset{\sim}{r}_j = e_j \left(\underset{\sim}{E} + \frac{1}{c} \frac{d}{dt} \underset{\sim}{r}_j \times \underset{\sim}{B}\right) , \tag{7}$$

where $\underset{\sim}{r}_j = (x_j, y_j)$ is the position coordinate for a particle of species j and $\underset{\sim}{E}$ and $\underset{\sim}{B}$ are the total electric and magnetic fields, and $m_j = \gamma_b m$ is the relativistic mass. Assuming $\underset{\sim}{E}$ and $\underset{\sim}{B}$ can be approximated by their equilibrium values, we substitute Eqs. (3) and (4) into Eq. (7). The equation of motion for the x direction can be expressed as

$$m_j \frac{d^2}{dt^2} x_j = 2\pi e_j \sum_k \hat{n}_k e_k (1 - \beta_j \beta_k)(x_j - X_k) . \tag{8}$$

Neglecting momentum spread, Eq. (8) can be averaged over the beam cross section. After some straightforward algebra, we obtain the approximate equation for average motion on the x direction,

$$m_j \frac{d^2}{dt^2} X_j = 2\pi e_j \sum_k \hat{n}_k e_k (1 - \beta_j \beta_k)(X_j - X_k) . \tag{9}$$

Similarly, the equation for average motion in the y direction is given by

$$m_j \frac{d^2}{dt^2} Y_j = 2\pi e_j \sum_k \hat{n}_k e_k (1 - \beta_j \beta_k)(Y_j - Y_k) . \tag{10}$$

Defining

$$Z_j = X_j + iY_j \tag{11}$$

and making use of Eqs. (9) and (10), we obtain

$$\frac{d^2}{dt^2} Z_j = \frac{2\pi e_j}{m_j} \sum_k \hat{n}_k e_k (1 - \beta_j \beta_k)(Z_j - Z_k) . \tag{12}$$

We seek oscillatory wave solutions to Eq. (12) of the form

$$Z_j = \hat{Z}_j \exp\{i[k_z(z + \beta_j c\, t) - \omega t]\} \tag{13}$$

where ω is the complex eigenfrequency, $\hat{Z}_j$ = const is the perturbed amplitude, and the axial wavenumber k_z is limited to the range

$$k_z^2 R_b^2 \lesssim 1 \quad . \tag{14}$$

Equation (14) assures the approximate validity of Eq. (12) for wave perturbations with $\partial/\partial z \neq 0$. Substituting Eq. (13) into Eq. (12), we obtain

$$\left[(\omega - k_z\beta_j c)^2 + \frac{2\pi e_j}{m_j}\sum_k \hat{n}_k e_k(1-\beta_j\beta_k)\right]\hat{Z}_j = \frac{2\pi e_j}{m_j}\sum_k \hat{n}_k e_k(1-\beta_j\beta_k)\,\hat{Z}_k \quad . \tag{15}$$

Equation (15) gives two homogeneous equations relating the amplitudes $\hat{Z}_e$ and $\hat{Z}_p$. Setting the determinant of the coefficients of $\hat{Z}_j$ equal to zero gives 2×2 matrix dispersion equation that determines the complex eigenfrequency ω. After some straightforward algebra, we obtain the dispersion relation

$$\left[(\omega + k_z c)^2 - \omega_{pe}^2\,(\hat{n}_p/\hat{n}_e)\right]\left[(\omega - k_z c)^2 - \omega_{pe}^2\right] \simeq \omega_{pe}^4\,(\hat{n}_p/\hat{n}_e) \quad , \tag{16}$$

where $\omega_{pe}^2 = 4\pi e^2\hat{n}_e/\gamma_b m$ is the electron plasma frequency-squared and use has been made of $\beta_e = -\beta_e \simeq 1$, which is consistent with present experimental parameters.

Assuming that both electron and positron beams have the same density,

and defining

$$a = k_z c + \omega_{pe} , \qquad b = k_z c - \omega_{pe} , \tag{17}$$

we simplify the dispersion relation in Eq. (16) as

$$(\omega^2 - a^2)(\omega^2 - b^2) = \omega_{pe}^4 , \tag{18}$$

which provides a necessary and sufficient condition

$$\omega_{pe}^4 > a^2 b^2 = (k_z^2 c^2 - \omega_{pe}^2)^2 \tag{19}$$

for instability. For the unstable branch, the perturbation is purely growing with the growth rate

$$\omega_i = Im\omega = \left\{\left(\frac{a^2 - b^2}{2}\right)^2 + \omega_{pe}^4\right\}^{1/2} - \frac{a^2 + b^2}{2}\Bigg\}^{1/2} . \tag{20}$$

The maximum growth rate of instability can occur at a=0 or b=0, thereby giving

$$(\omega_i)_m = (5^{1/2} - 2)^{1/2} \omega_{pe} \simeq 0.5\ \omega_{pe} . \tag{21}$$

For colliding beams interacting over a finite distance L, the axial wavenumber k_z is $k_z = 2\pi n/L$ where $n = 1, 2, \ldots$. In this case, the condition for a=0 becomes $L\omega_{pe}/c = 2\pi n$. The finite interaction length also imposes a severe condition for the instability to grow significantly before the beam exit. Although a small growth of perturbations during one individual

interaction of electron and positron beams, we expect that due to this filamentation instability, the repating interactions between both beams eventually convert the longitudinal energy of the beams into the transverse energy of beams and the field energy of perturbations, thereby broadening the beam cross section and leading to reduction of luminosity. However, the analysis of broadening of beam cross section is particularly difficult and is currently under investigation by the authors.

B. Vlasov Description

In the previous section, we have investigated the stability properties of dipole oscillation in the transverse instability for the electron and positron colliding beams, within the context of rigid beam model. Although a dipole oscillation in a rigid beam model provides a simple instructive description, it is necessary to investigate stability properties for perturbations with high azimuthal harmonic number $\ell \geq 2$ within the framework of the Vlasov-Maxwell equations.

For beams of well-defined energy and momentum, an equilibrium associated with the steady-state ($\partial/\partial t=0$) beam distribution function,

$$f_j^o(H,P_\theta,P_z) = \frac{\hat{n}_j}{2\pi\gamma_b m} \delta(H-\omega_j P_\theta-\hat{\gamma}_j mc^2)\delta(P_z-\gamma_b m\beta_j c) \ , \tag{22}$$

is particularly suited for stability analysis, where the total energy,

$$H = (m^2c^4 + c^2p^2) + e_j\phi_o(r) \ , \tag{23}$$

the canonical angular momentum,

$$P_\theta = rp_\theta \ , \tag{24}$$

and the axial canonical momentum

$$P_z = p_z + (e_j/c)A_z^s(r) \ , \tag{25}$$

are the three single-particle constants of the motion in the equilibrium fields, and ω_j is the beam rotational frequency of species j and $\hat{\gamma}_j$ is a constant. In Eqs. (23)-(25), $\phi_o(r)$ is the equilibrium self-electric potential, $A_z^s(r)$ is the axial component of vector potential for the azimuthal self-magnetic field, and $\underset{\sim}{p} = (p_r, p_\theta, p_z)$ denotes mechanical momentum and is related to the particle velocity $\underset{\sim}{v}$ by $\underset{\sim}{v} = (\underset{\sim}{p}/m)(1+\underset{\sim}{p}^2/m^2c^2)^{-1/2}$.

Since the r-θ kinetic energy of particles is small in comparison with the characteristic energy $\gamma_b mc^2$, it is straightforward to show that the term $H-\omega_j P_\theta$ in Eq. (22) can be approximated by[7]

$$H - \omega_j P_\theta = \gamma_b mc^2 + \frac{p_\perp^2}{2\gamma_b m} + \frac{1}{2}\gamma_b m\omega_j^2 r^2 \ , \tag{26}$$

where

$$\gamma_b^2 = (1-\beta_p^2)^{-1}, \quad p_\perp^2 = p_r^2 + (p_\theta - \gamma_b m\omega_j r)^2 \ ,$$

and

$$\Omega_j^2 = (\hat{\omega}_j - \omega_j)(\omega_j + \hat{\omega}_j) = -\omega_j^2 - \frac{2\pi e_j}{\gamma_b m}\sum_k \hat{n}_k e_k(1-\beta_j\beta_k) \ . \tag{27}$$

In Eq. (27), the laminar rotation frequency $\hat{\omega}_j$ is defined by

$$\omega_j = \left[- \frac{2\pi e_j}{\gamma_b m} \sum_k \hat{n}_k e_k \left(1-\beta_j\beta_k\right)\right]^{1/2} . \tag{28}$$

Substituting Eq. (26) into Eq. (22), we find the equilibrium particle density profile

$$\begin{aligned} n_j^o(r) &= \int d^3p\, f_j^o(H,P_\theta,P_z) \\ &= \begin{cases} \hat{n}_j , & 0<r<R_b , \\ 0 , & \text{otherwise,} \end{cases} \end{aligned} \tag{29}$$

where the beam radius R_b is defined by

$$R_b^2 = 2c^2\left(\hat{\gamma}_j-\gamma_b\right)/\gamma_b\Omega_j^2 \tag{30}$$

for j=e,p. Equation(30) ensures that the electron and positron beams have the common beam radius R_b. It is important to note from Eqs. (27) and (30) that the radially confined equilibrium exists only for the rotational frequency ω_j satisfying

$$-\hat{\omega}_j < \hat{\omega}_j < \hat{\omega}_j . \tag{31}$$

Additional equilibriium properties associated with the distribution function in Eq. (22) are discussed in Ref. 7.

In order to obtain the dispersion relation for filamentation instability of the electron and positron beams, we make use of the linearized Vlasov-Maxwell equations. For perturbations with azimuthal

harmonic number ℓ and axial wavenumber k_z, a perturbed quantity $\delta\phi(\underset{\sim}{x},t)$ can be expressed as $\delta\phi(\underset{\sim}{x},t)=\hat{\phi}(r)\exp\{i(\ell\theta+k_z z-\omega t)\}$, where ω is the complex eigenfrequency. The present stability analysis is carried out in long parallel wavelength and low frequency perturbation satisfying $k_z^2 R_b^2 << \ell^2+1$, $|\omega R_b/c|^2 << \ell^2+1$. With this assmption, the axial components of perturbed field $E_z(r)$ and $B_z(r)$ are negligible and the Maxwell equations of perturbed potentials can be expressed as

$$\left(\frac{1}{r}\frac{\partial}{\partial r}\, r\,\frac{\partial}{\partial r} - \frac{\ell^2}{r^2}\right)\hat{\phi}(r) = -4\pi\hat{\rho}(r) \tag{32}$$

and

$$\left(\frac{1}{r}\frac{\partial}{\partial r}\, r\,\frac{\partial}{\partial r} - \frac{\ell^2}{r^2}\right)\hat{A}(r) = -\frac{4\pi}{c}\hat{J}_z(r) \tag{33}$$

where $\hat{\phi}(r)$ is the perturbed electrostatic potential, $\hat{\rho}(r)$ is the perturbed charge density, $\hat{A}(r)$ and $\hat{J}_z(r)$ are the axial components of the perturbed vector potential and current density, respectively. Components of perturbed fields can be expressed in terms of $\hat{\phi}(r)$ and $\hat{A}(r)$ as $\hat{E}_\theta = -i\ell\hat{\phi}(r)/r$, $\hat{E}_r(r) = -(\partial/\partial r)\hat{\phi}(r)$, $\hat{B}_r(r) = i\ell\hat{A}(r)/r$, and $\hat{B}_\theta(r) = -(\partial/\partial r)\hat{A}(r)$.

In order to calculate perturbed charge and current densities, we solve the linearized Vlasov equation to obtain the perturbed distribution function[7]

$$\begin{aligned}\hat{f}_j(r,p) = \frac{e_j\gamma_b m}{p_\perp}\frac{\partial f_j^0}{\partial p_\perp}\Big\{&\hat{\psi}_j(r) + (\omega-\ell\omega_j-k_z\beta_j c)\\ &\times\int_{-\infty}^{0} d\tau\; i\,\hat{\psi}_j(r')\exp[i\,\ell(\theta'-\theta)-i(\omega-k_z\beta_j c)\tau]\Big\},\end{aligned} \tag{34}$$

where the perturbed electrostatic potential $\hat{\psi}_j(r)$ in the frame of reference moving with velocity $\beta_j c$ is defined by $\hat{\psi}_j(r)=\hat{\phi}(r)-\beta_j\hat{A}(r)$ and use has been made of $p_z/\gamma_b m=\omega_j$ consistent with Eq. (1). It is useful to introduce the polar momentum variables $(p_\perp,\phi)$ in the rotating frame defined by $p_x + \gamma_b m\omega_j y = p_\perp \cos\phi$, $p_y - \gamma_b m\omega_j x = p_\perp \sin\phi$. Note also that the Cartesian coordinates (x,y) are related to the polar coordinates (r,θ) by x=r cosθ and y=r sinθ. In this context, the transverse equation of motion of particles can be expressed as[7]

$$x'(\tau) = (1/\hat{\omega}_j)[(p_\perp/\gamma_b m)\cos\phi \sin\hat{\omega}_j\tau - r\omega_j\sin\theta\sin\hat{\omega}_j\tau + r\hat{\omega}_j\cos\theta\cos\hat{\omega}_j\tau]$$

$$y'(\tau) = (1/\hat{\omega}_j)[(p_\perp/\gamma_b m)\sin\phi\sin\hat{\omega}_j\tau + r\hat{\omega}_j\cos\theta\sin\hat{\omega}_j\tau + r\hat{\omega}_j\sin\theta\cos\hat{\omega}_j\tau]. \tag{35}$$

where $\tau=t'-t$, and the harmonic frequency $\hat{\omega}_j$ is defined in Eq. (28).

Upon integration of Eq. (34), the perturbed charge density can be found to be

$$\hat{\rho}(r) = 2\pi e^2 \sum_j \gamma_b m \int_0^\infty dp_\perp\, p_\perp \int_{-\infty}^{\infty} dp_z \frac{1}{p_\perp}\frac{f_j^o}{p_\perp}[\hat{\psi}_j(r) + (\omega-\ell\omega_j-k_z\beta_j c)\hat{I}_j] . \tag{36}$$

where the orbit integral $\hat{I}_j$ is defined by

$$I_j = i\int_0^{2\pi}\frac{d\phi}{2\pi}\int_{-\infty}^{0} d\tau\, \hat{\psi}_j(r')\exp\{i[\ell(\theta'-\theta)-(\omega-k_z\beta_j c)\tau]\} . \tag{37}$$

Similarly the perturbed axial current density can be obtained. For analytic traceability, we will consider here a class of special solutions

for which the perturbed charge and current density are localized on the beam surface, i.e., equal to zero except at $r=R_b$. More general perturbations, particularly the body wave perturbations, are to be presented in a subsequent publication. In this case, it follows from Eqs. (32) and (33) that the function $\psi_j(r)$ has the simple form $\hat{\psi}_j(r) = \hat{\phi}(r) - \beta_j \hat{A}(r) = C_j r^{\ell}$ for $0<r<R_b$. Substituting Eq. (35) into Eq. (37) it is readily shown that

$$I_j = \frac{i\hat{\psi}_j(r)}{(2\omega_j)^{\ell}} \int_{-\infty}^{0} dt \exp[-i(\omega - k_z \beta_j c)t] \{[(\omega_j+\omega_j)\exp(i\omega_j t) - (\omega_j-\omega_j)\exp(-i\omega_j t)]^{\ell} \quad . \tag{38}$$

After some straightforward algebra that utilizes Eqs. (22), (36) and (38), Eq. (32) can be expressed as

$$\left(\frac{1}{r}\frac{\partial}{\partial r} r \frac{\partial}{\partial r} - \frac{\ell^2}{r^2}\right)\hat{\phi}(r) = -\sum_j \hat{\psi}_j(r) \frac{\omega_{pj}^2}{\Omega_j^2 R_b} \Gamma_j(\omega)\, \delta(r-R_b) \quad , \tag{39}$$

where $\omega_{pj}^2 = 4\pi e^2 \hat{n}_j / \gamma_b m$ is the plasma frequency - squared of beam component j, $\Omega_j^2 = (\hat{\omega}_j - \omega_j)(\omega_j + \hat{\omega}_j)$ is defined in Eq. (27) and $\Gamma_j(\omega)$ is defined by

$$\Gamma_j(\omega) = -1 + \left(\frac{\hat{\omega}_j - \omega_j}{2\hat{\omega}_j}\right)^{\ell} \sum_{n=0}^{\ell} \frac{\ell!}{n!(\ell-n)!} \frac{\omega - \hat{\omega}_j - k_z \beta_j c}{\omega - k_z \beta_j c + \hat{\omega}_j - 2n\hat{\omega}_j} \left(\frac{\omega_j + \hat{\omega}_j}{\omega_j - \omega_j}\right)^n \tag{40}$$

Similarly, Eq. (33) can be expressed as

$$\left(\frac{1}{r}\frac{\partial}{\partial r} r \frac{\partial}{\partial r} - \frac{\ell^2}{r^2}\right)\hat{A}(r) = -\sum_j \beta_j \hat{\psi}_j(r) \frac{\omega_{pj}^2}{\Omega_j^2 R_b} \Gamma_j(\omega)\delta(r-R_b) \quad . \tag{41}$$

where use has been again made of the approximation $p_z/\gamma_b m \simeq \beta_j c$ consistent with Eq. (1).

As the right-hand sides of the coupled differential equations (39) and (41) are equal to zero except at the surface of the beam $r=R_b$, they can be solved in a straightforward manner to give

$$C_k = \sum_j (1-\beta_k\beta_j) \frac{\omega_{pj}^2}{2\ell\Omega_j^2} \Gamma_j(\omega) C_j \ . \tag{42}$$

In the case when the beams are located inside the cylindrical conducting wall with radius R_c, the term C_k in the left-hand side of Eq. (42) is replaced by $[1-(R_b/R_c)^2]^{-1}C_k$. Note that the absolute value of $\omega_{p_j}^2\Gamma_j(\omega)/\Omega_j^2$ in Eq. (42) is of the order of unity or less. It follows from Eq. (42) that the condition for a nontrivial solution (C_j not all zero) is given by

$$1 - (\omega_{pp}^2\ \omega_{pe}^2/\ell^2\ \Omega_p^2\ \Omega_e^2)\ \Gamma_p(\omega)\ \Gamma_e(\omega) = 0 \ , \tag{43}$$

where use has been made of $\beta_p=-\beta_e\simeq 1$ and $\gamma_b^{-2}<<1$, which is consistent with present experimental parameters. Equation (42), when combined with Eq. (40), constitutes one of the main results of this paper and can be used to investigate filamentation stability properties for a broad range of system parameters.

As an example, we restrict the investigation of dispersion relation (43) to the case, where both beams are in a cold fluid rotational equilibrium characterized by $\omega_j \to \pm\hat{\omega}_j$. A careful examination of expression for $\Gamma_j(\omega)$ show that[7]

$$\lim_{\omega_j\to\pm\hat{\omega}_j} \left[\frac{\omega_{pj}^2}{2\ell\Omega_j^2}\Gamma_j(\omega)\right] = \frac{\omega_{pj}^2}{2(\omega-k_z\beta_j c\mp\ell\hat{\omega}_j)[\omega-k_z\beta_j c\mp(\ell-2)\hat{\omega}_j]} \tag{44}$$

Therefore, in a cold fluid limit, the dispersion relation in Eq. (43) can be considerably simplified. After some algebraic manipulation we can show that for the fundamental mode perturbation (i.e., $\ell=1$), the dispersion relation in Eq. (43) is identical to Eq. (16) obtained within the framework of rigid beam model. The stability analysis of Eq. (43) for a broad range of harmonic number ℓ and rotational frequency ω_j is currently under investigation by the authors. Nonlinearly the beams become filamentated first, then the current filaments of the same sign attract each other to form a broader beam. Finally, we conclude this section by pointing out that the understanding in broadening in beam cross section by repeating interactions of beams is not completed yet. And this area is currently under investigation by the authors.

III. COLLECTIVE SELF-FIELD EFFECTS

In this section, we examine the influence of the collective self-fields[5] on the electron and positron colliding beams in the storage ring. While the forces of the self-generated electric and magnetic field of a highly relativistic electron (positron) beam on an electron (positron) cancel out to order $0(\gamma^{-2})$, i.e., $E_r + \beta_c B_\theta \approx 0(\gamma^{-2})$ the forces of the electric and magnetic fields of the electron beam on the colliding positrons are additive leading to radial acceleration. This effect of the collective self-fields of one species on the other species of the colliding beams imparts considerable transverse energy, thereby substantially increasing the beam transverse dimensions upon collision. In order to make the problem simple, we assume that the colliding section of the storage ring is straight. The theoretical analysis is carried out, distinguishing the two cases, where (a) the particle motions are in a very coherent orbit and (b) the randomness dominates the operational condition of storage ring (e.g., incoherent collision location by fluctuation, etc.). In either case, it is found that the self-fields effects play a dominant role in the stability behavior of transverse orbit or the expansion of beam cross section. For present experimental parameters[4] at DESY, the cross section of the beam can be expanded to ten times of its original area within 5 milliseconds operational time. Without loss of generality, we assume in Fig. 1 that the front edges of both beams arrive in z=0 at time t=0.

The axial orbit of particles of beam component j is given by

$$z = z_j + v_j t \tag{45}$$

where the initial position z_j is restricted to satisfy

$$z_j(z_j + \ell_j) < 0 . \tag{46}$$

Here $\varepsilon_j = \text{sgn } e_j$ and e_j is the charge of the particles of beam component j. The particle density profile of beam component j is expressed as

$$n_j^o(r,z,t) = n_j(r,z)U[(\beta_j ct-z)(z+\varepsilon_j L-\beta_j ct)] \ , \tag{47}$$

where the Heaviside step function U(x) is defined by

$$U(x) = \begin{cases} 0, & x<0 \ , \\ 1, & x>0 \ . \end{cases} \tag{48}$$

For a specific choice of the beam density $n_j(r,z)$ in Eq. (47), the potentials for the self-fields are to be calculated from the Maxwell equations. The Poisson equation can be approximated by

$$\frac{1}{r}\frac{\partial}{\partial r} r \frac{\partial}{\partial r} \phi(r,z,t) = - 4\pi \sum_j e_j n_j^o(r,z,t) \ , \tag{49}$$

where $\phi(r,z,t)$ is the self-electric potential. In obtaining Eq. (49), we neglect the term proportional to $\partial^2\phi/\partial^2 z$, under the assumption that the axial length L of the beam is much larger than the beam radius and the effects of the leading edge of the beams are thus neglected. Furthermore, the z-component of the $\nabla \times \underset{\sim}{B}^s(\underset{\sim}{x})$ Maxwell equation is expressed as

$$\frac{1}{r}\frac{\partial}{\partial r} r \frac{\partial}{\partial r} A_z^s(r,z,t) = - 4\pi \sum_j e_j \beta_j n_j^o(r,z,t) \ , \tag{50}$$

where $A_z^s(r,z,t)$ is the z-component of the self-vector potential. Other components of the vector potential are negligible because of Eq. (1). Defining the effective self-potential $\psi_j^s(r,z,z_j) = \phi - \beta_j A_z^s$, and making use of Eqs. (45) (47), (49), and (50), we have

$$\frac{\partial}{\partial r}\psi_j^s(r,z,z_j) = - 8\pi e_k \frac{1}{r}\int_o^r dr' r' n_k(r',z) \tag{51}$$

$$\times U[(z_j-2z)(2z-z_j+\varepsilon_k L)] \ ,$$

where $k \neq j$. In obtaining Eq. (51), use has been made of $\gamma_b^{-2} = (1-\beta_p^2) << 1$.

In order to make the problem simple, we carry out the analysis in the average applied field provided externally by the periodic quadrupole magnetic field, similar to that used in the previous study[6]. In this regard, the applied focussing force can be obtained from the axial component of the effective vector potential

$$A_z^{ext}(r) = -(\gamma_b m/2e\beta_p)\ \omega_f^2 r^2 \tag{52}$$

where ω_f is the focussing oscillation frequency determined by the quadrupole field gradient.

The total energy of particles of the beam component j is given by

$$H = (m^2c^4 + c^2 \underset{\sim}{p}^2)^{1/2} + e_j\phi(r,z,t), \tag{53}$$

where the lower case p denotes mechanical momentum and is related to the particle velocity $\underset{\sim}{v}$ by $\underset{\sim}{v} = \underset{\sim}{p}/m(1+\underset{\sim}{p}^2/m^2c^2)^{1/2}$. Since the r-$\theta$ kinetic energy of particles is small in comparison with the characteristic energy $\gamma_b mc^2$ and $\nu_j/\gamma_b << 1$ in Eq. (1), it is straightforward to show that Eq. (53) can be approximated by

$$H = \gamma_b mc^2 + \frac{p_x^2+p_y^2}{2\gamma_b m} + e_j\psi_j^s(r,z,z_j) + \frac{1}{2}\gamma_b m\ \omega_f^2\ r^2\ , \tag{54}$$

where $\gamma_b^2 = (1-\beta_j^2)^{-1}$. From Eq. (54), we obtain the equation of motion for

$$Z(t) = x(t) + iy(t) \tag{55}$$

where $i = (-1)^{1/2}$. Making use of Eqs. (45) and (55), and $\beta_j^2 \simeq 1$, the equation of motion for particles of the beam component j is given by

$$\frac{d^2Z}{dz^2} + \frac{8\pi e^2}{\gamma_b mc^2} \cdot \frac{Z}{r^2} \int_o^r dr'r'n_k(r',z)U[(z_j-2z)(2z-z_j+\varepsilon_k L)] + \frac{\omega_f^2}{c^2} Z = 0 \tag{56}$$

where $k \neq j$ and z_j is defined in Eq. (45). Equation (56) determines the transverse position of particles of beam component j, thereby providing the information of the particle density $n_j(r,z)$, which in turn governs the equations of motion for particles of the beam component k. In this regard, the coupled differential equation (56) for j=e and p can be used to investigate the temporal profile evolutions of various beam properties for a broad range of initial parameters.

As an example, we consider a tenuous positron beam satisfying

$$\bar{\omega}_{pp}^2 << (c/L)^2 , \tag{57}$$

where $\bar{\omega}_{pp}^2 = 4\pi\bar{n}_p e^2/\gamma_b m$ is the average positron plasma frequency-squared in the laboratory frame. Equation (57) assures that all the electrons move on the straight paths with constant radius r during the collision. Assuming the electron density profile as

$$n_e(r,z) = \begin{cases} \hat{n}_e , & r<R_b , \\ 0 , & \text{otherwise,} \end{cases} \tag{58}$$

the transverse equation of motion for positron can be expressed as

$$\frac{d^2 Z}{dz^2} + \frac{\omega_{pe}^2}{c^2} Z\, U[(z_p-2z)(2z-z_p-L)] + \frac{\omega_f^2}{c^2} Z = 0 , \tag{59}$$

where $\omega_{pe}^2 = 4\pi\hat{n}_e e^2/\gamma_b m$ is the electron plasma frequency-squared.

Without loss of generality, we assume that there is one pair of electron and positron beams in the entire system, thereby indicating that the whole storage ring can be represented by two focusing sectors. Each sector consists of a self-beam focusing set (the region in which beams collide) and an applied focusing set. The subsequent analysis is carried out distinguishing the two cases: (a) the positrons move on a very coherent orbit, and (b) the

axial location of collision as well as the beam length fluctuates incoherently, thereby the ensemble average can be feasible.

A. Stability Analysis of Coherent Positron Orbit

The stability properties of individual particle orbit can be determined from the transformation matrix of one sector[8] for a very coherent positron orbit. Assuming that a positron has an initial condition $Z=Z_1$ and $Z' = (dZ/dz) = Z_1'$ at $z = z_p/2$, it can be shown from Eq. (59) that the transverse orbit of this positron is given by

$$Z = Z_1\cos[(\omega_T/c)(z-z_p/2)] + (Z_1'c/\omega_T)\sin[(\omega_T/c)(z-z_p/2)] \ , \qquad (60)$$

for $z_p/2<z<z_p/2+L$. Here the frequency $\omega_T = (\omega_{pe}^2 + \omega_f^2)^{1/2}$. From Eq. (60) it is also straightforward to show that the transverse position Z_2 and orbit slope Z_2' of positron, when it emerges from the right-hand side of the electron beam, is given by

$$\begin{pmatrix} Z_2 \\ Z_2' \end{pmatrix} = \begin{pmatrix} \cos(\omega_T L/2c) & (c/\omega_T)\sin(\omega_T L/2c) \\ -(\omega_T/c)\sin(\omega_T L/2c) & \cos(\omega_T L/2c) \end{pmatrix} \begin{pmatrix} Z_1 \\ Z_1' \end{pmatrix} \qquad (61)$$

Similarly, when the applied focusing section has been traversed, the position and orbit slope are given by

$$\begin{pmatrix} Z_3 \\ Z_3' \end{pmatrix} = \begin{pmatrix} \cos\Phi & (c/\omega_f)\sin\Phi \\ -(\omega_f/c)\sin\Phi & \cos\Phi \end{pmatrix} \begin{pmatrix} Z_2 \\ Z_2' \end{pmatrix} \qquad (62)$$

where the phase shift $\Phi = \omega_f(S-L)/2c$ and S is the length of the whole circumference of storage ring.

Therefore, from Eqs. (61) and (62), we obtain the trace of the transformation matrix M for a sector

$$\mathrm{Tr}\,M = 2\cos\phi\,\cos\left(\frac{\omega_T L}{2c}\right) - \left(\frac{\omega_T}{\omega_f} + \frac{\omega_f}{\omega_T}\right)\sin\phi\,\sin\left(\frac{\omega_T L}{2c}\right) , \tag{63}$$

which is the sum of the elements of the principal diagonal of the transformation matrix M. The necessary and sufficient condition for stable transverse orbit is[8]

$$\left|\frac{1}{2}\,\mathrm{Tr}\,M\right| \leq 1 . \tag{64}$$

As a typical example in the present experiment,[4] we consider the system parameters $\omega_{pe} = 10^9$ rad/sec, $L = 2$cm, and $\omega_f = 2\times10^7$ rad/sec. Substituting these parameters into Eq. (63) gives approximately $\mathrm{Tr}\,M/2 \simeq \cos\phi - \sin\phi$, which violates the inequality in Eq. (64) for the range $(n-0.5)\pi < \phi < n\pi$, where n is an integer. We therefore conclude that the collective self-fields effects (ω_{pe}) of the electron and positron colliding beams play a significant role in the stability behavior of transverse particle orbit.

B. Expansion of Beam Cross Section with Ensemble Average

In order to investigate the expansion of beam cross section for uncontrollable collision (incoherent collision location, etc.), we define

$$r_1^2 = Z_1 Z_1^* + (c/\omega_f)^2 Z_1' Z_1'^* , \tag{65}$$

which represents the maximum radial deviation from the axis of symmetry before collision. In Eq. (65), the asterisk (*) denotes the complex conjugate. During the collision ($z_p/2 < z < z_p/2 + L$), the transverse orbit of a positron in Eq. (60) can also be expressed as

$$Z = A\cos[(\omega_T/c)(z - z_p/2) + \alpha] , \tag{66}$$

where A is the maximum amplitude and α is the initial phase angle which is

defined by $\alpha = \tan^{-1}[-(c/\omega_T)Z_1'/Z_1]$. The maximum radial deviation for range z satisfying $z_p/2 < z < z_p/2 + L$ is determined from

$$AA^* = r_1^2/[1 + (\omega_{pe}/\omega_f)^2 \sin^2\alpha] \ , \tag{67}$$

where use has been made of Eqs. (65) and (66), and $\omega_T = (\omega_{pe} + \omega_f^2)^{1/2}$. From Eq. (66), the positron position Z_2 and orbit slope Z_2' can be expressed as

$$Z_2 = A \cos[(\omega_T L/2c) + \alpha] \ ,$$

$$Z_2' = -A(\omega_T/c)\sin[(\omega_T L/2c) + \alpha] \ ,$$

thereby giving the relation

$$\left(\frac{r_2}{r_1}\right)^2 = \frac{1+(\omega_{pe}/\omega_f)^2 \sin^2[(\omega_T L/2c)+\alpha]}{1+(\omega_{pe}/\omega_f)^2 \sin^2\alpha} \ , \tag{68}$$

from which the maximum radial deviation r_2 after collision is determined.

Depending on the phase angle α, positrons gain (or lose) the transverse energy by the collision according to $r_2/r_1 > 1$ (or $r_2/r_1 < 1$). The net gain of the transverse energy (or temperature) by the collision is determined from the phase angle average of Eq. (68). We therefore define

$$\langle r_2^2/r_1^2 \rangle = \frac{1}{2\pi} \int_0^{2\pi} d\alpha \ \frac{1+(\omega_{pe}/\omega_f)^2 \sin^2[(\omega_T L/2c)+\alpha]}{1+(\omega_{pe}/\omega_f)^2 \sin^2\alpha} \ f(\alpha) \tag{69}$$

for future notational convenience. In Eq. (69), the phase angle distribution $f(\alpha)$ is a positive definite function normalized by $\int_0^{2\pi} d\alpha \, f(\alpha) = 2\pi$. For uniform distribution (f=1), we obtain

$$\langle r_2^2/r_1^2 \rangle = \cos\left(\frac{\omega_T L}{c}\right) + \frac{1+\omega_{pe}^2/2\omega_f^2}{(1+\omega_{pe}^2/\omega_f^2)^{1/2}} \left[1-\cos\left(\frac{\omega_T L}{c}\right)\right] . \tag{70}$$

Evidently, we note from Eq. (70) that the value $\langle r_2^2/r_1^2 \rangle$ approaches unity

when the beam length (L) or density (ω_{pe}) decreases to zero. Moreover, the value $\langle r_2^2/r_1^2\rangle$ is always greater than unity.

As a typical example in the present experiment, we evaluate Eq.(70) for $\omega_{pe} = 10^9$ rad/sec, L = 2cm and $\omega_f = 2\times10^7$ rad/sec. Substituting these parameters into Eq. (70), we find $\langle r_2^2/r_1^2\rangle \simeq 1.025$. Therefore, in these particular parameters, the cross section of the beam is increased by 2.5 percent of its original area after each collision. However, we assume that the positrons are uniformly distributed in the phase angle α whenever beams start collision, which is consistent with the ensemble average scheme. The cross section of the positron beam can be expanded to ten times of its original area for $\langle r_2^2/r_1^2\rangle = 1.025$ after 100 times collisions, which corresponds to the operational time $(S/2c)\log 1.025 = 5$ milliseconds for the circumferential legnth $S = 3\times10^6$cm of storage ring.

IV. CONCLUSIONS

In this paper, we have examined the filamentation instability and the influence of the collective self-fields on the electron-positron colliding beams in the storage ring. In Sec. II, we have investigated the stability properties of filamentation instability of electron-positron colliding beam. An important conclusion of this stability analysis is that the typical growth rate of the filamentation instability is order of the electron plasma frequency, thereby severely limiting the electron density in a storage ring. Influence of collective self-field effects on the electron and positron colliding beams has been investigated in Sec. III. The theoretical analysis has been carried out, distinguishing the two cases, where (a) the particle motions are in a very coherent orbit and (b) the randomness dominates the operational condition of storage ring (e.g., incoherent collision location by fluctuation, etc.). In either case, it has been found that the self-fields effects play a dominant role in the stability behavior of transverse orbit and the expansion of beam cross section.

ACKNOWLEDGMENTS

We wish to thank Professor Ming Chen and Professor Gus Zorn for informing us about the experimental observation of beam broadening at DESY, and Professor R. C. Davidson for useful discussions. This work was supported in part by the Independent Research Fund at the Naval Surface Weapons Center and in part by the Office of Naval Research under the auspices of a University of Maryland-Naval Research Laboratory joint program (Contract N-00014-77-C-0590).

REFERENCES

1. J. R. Rees, IEEE Trans. Nucl. Sci. NS-24, 1836 (1977).
2. G. A. Voss, IEEE Trans. Nucl. Sci. NS-24, 1842 (1977).
3. H. S. Uhm and C. S. Liu, Phys. Rev. Lett. 43, 914 (1979).
4. G. A. Voss, Bull. Am. Phys. Soc. 24, 142 (1979).
5. H. S. Uhm and C. S. Liu, "Collective Self-Field Effects on the Electron and Positron Colliding Beams in Storage Ring," TR-79-112, Univ. of Maryland (1979).
6. R. L. Gluckstern, Proc. 1970 Proton Linac Conf., edited by N. R. Tracy, (Natinal Accelerator Lab., Batavia, Illinois, 1970), p. 811.
7. H. S. Uhm and R. C. Davidson, "Kinetic Description of Coupled Transverse Oscillations in an Intense Relativisitc Electron Beam-Plasma System," Phys. Fluids 23, 813, (1980).
8. J. J. Livingood, Principles of Cyclic Particle Accelerators, (D. Van Nostromd Company, Inc., Princeton, N.J., 1961), Chap. 3.

FIGURE CAPTION

Fig. 1 System configuration and coordinate system.

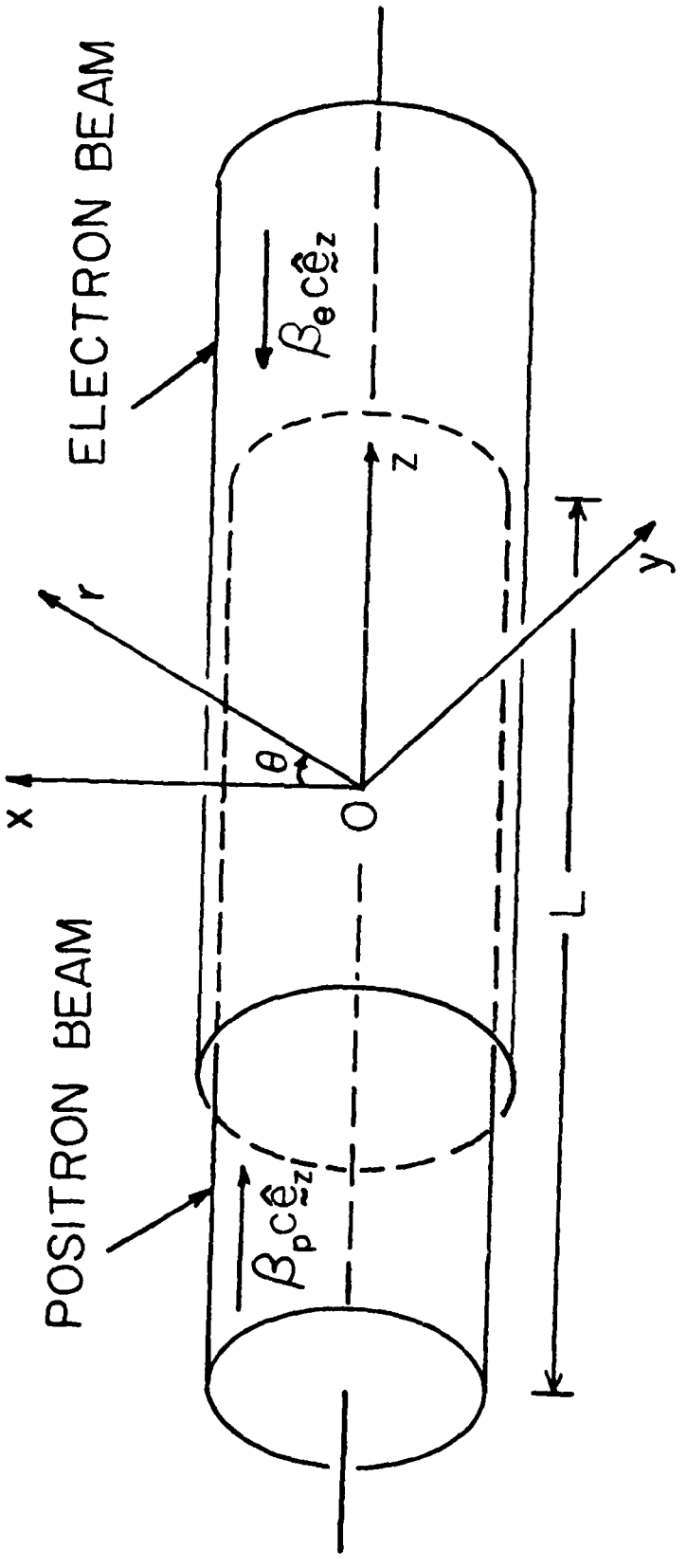
ELECTRON BEAM
$\beta_e c\hat{e}_z$
z
r
y
θ
x
O
L
POSITRON BEAM
$\beta_p c\hat{e}_{z'}$

Figure 1